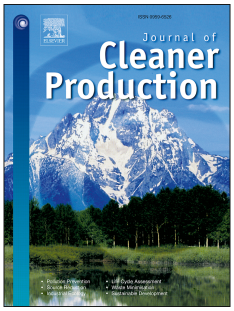

Conversion of tannery solid waste to sound absorbing nanofibrous materials: A road to sustainability

Sowmya Selvaraj, Vigneshwar Jeevan, Raghava Rao Jonnalagadda, Nishter Nishad Fathima

PII: S0959-6526(18)33854-X

DOI: https://doi.org/10.1016/j.jclepro.2018.12.144

Reference: JCLP 15202

To appear in: *Journal of Cleaner Production*

Received Date: 23 April 2018

Revised Date: 11 December 2018

Accepted Date: 15 December 2018

Please cite this article as: Selvaraj S, Jeevan V, Rao Jonnalagadda R, Nishad Fathima N, Conversion of tannery solid waste to sound absorbing nanofibrous materials: A road to sustainability, *Journal of Cleaner Production* (2019), doi: https://doi.org/10.1016/j.jclepro.2018.12.144.

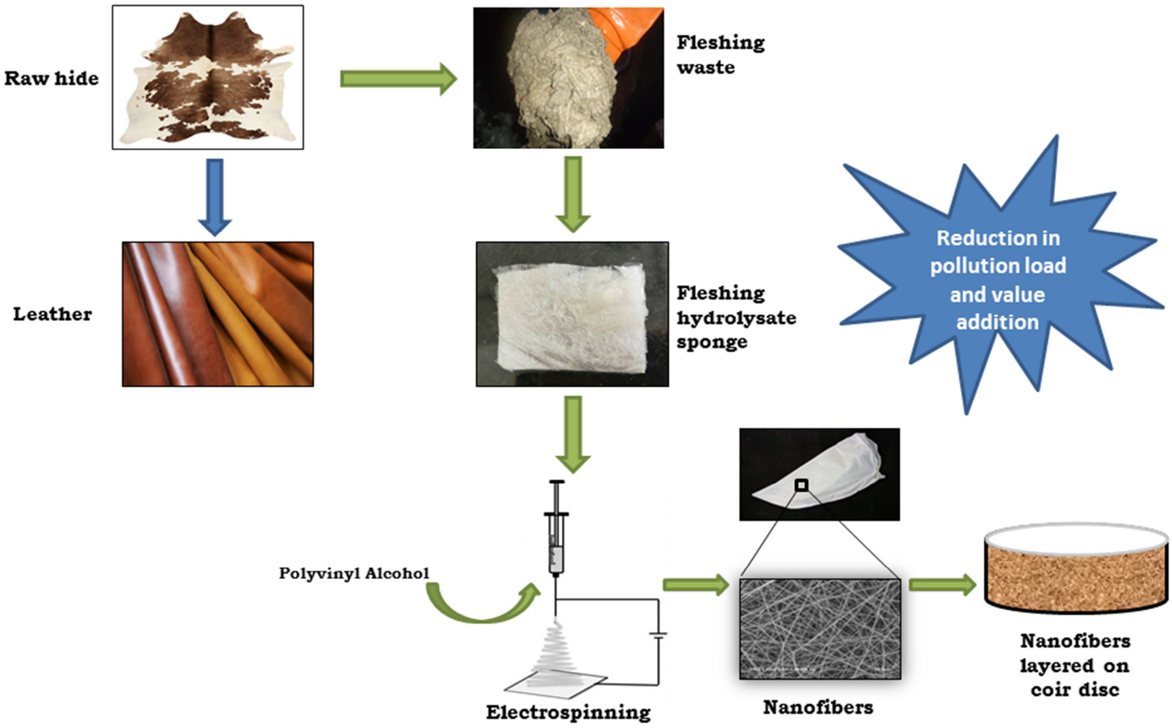
Raw hide
Fleshing waste
Leather
Fleshing hydrolysate sponge
Reduction in pollution load and value addition
Polyvinyl Alcohol
Electrospinning
Nanofibers
Nanofibers layered on coir disc

Conversion of tannery solid waste to sound absorbing nanofibrous materials: A road to sustainability

*Sowmya Selvaraj, Vigneshwar Jeevan, Raghava Rao Jonnalagadda, Nishter Nishad Fathima**

Inorganic and Physical Chemistry Laboratory, Council of Scientific and Industrial Research-Central Leather Research Institute, Adyar, Chennai, India- 600020

* Author for correspondence

Tel: +91 44 2443 7188, 2443 7137

Email: nishad@clri.res.in; nishad.naveed@gmail.com

ABSTRACT

Leather making process necessitates the effective utilization of potential waste from the meat industry through tanning. This results in the generation of solid wastes leading to serious environmental concerns. Fleshing waste is considered to be one of the major solid wastes, which contains proteins and fat. The current disposal methods of fleshing wastes have various challenges and limitations. In order to overcome these drawbacks/limitations, we propose a novel approach for converting fleshing waste into a value-added material for acoustics application. Herein, protein hydrolysate was prepared from the fleshing waste through acid hydrolysis and was blended with polyvinyl (alcohol) (PVA) to produce nanofibers through the electrospinning process by optimizing the electrospinning parameters. Acid hydrolysis was done at varying conditions and its effect on the properties of the nanofibers was studied. Nanofibers were characterized using scanning electron microscopy (SEM), differential scanning calorimetry (DSC) and x-ray diffraction (XRD) studies. The experimental observations indicated that the nanofibers produced with fleshing hydrolysate- PVA showed enhanced thermal stability than neat PVA nanofibers. The prepared nanofibrous membrane was placed on the natural sound absorbing material coir and the sound absorbing potential of this bilayer material was characterized. The sound absorption studies revealed that the bilayer material, which consisted of fleshing hydrolysate- PVA nanofibers with coir disc has better sound absorbing potential in the lower frequencies when compared to pure coir and PVA nanofibers with coir material. This gives new insights into the potential use of fleshing waste derived nanofibers as sound absorbing layer in acoustic applications.

KEYWORDS: Fleshing waste; leather; nanofibers; electrospinning and acoustics.

1.0 INTRODUCTION

Leather making process involves the conversion of animal hides/skin to a non-putrescible material called leather by subjecting them to various chemical and mechanical processes. Leather industry plays a significant role in the global economy because of the higher need for leather due to its fascinating properties over synthetic materials, which also helps in employing the weaker section of the society. However, the industry generates substantial quantities of solid and liquid wastes, which pose a serious threat to the environment. Processing of one metric ton of wet salted cow hide yields 200 kg of finished leather alongside 250 kg of tanned, 350 kg of non-tanned solid wastes with the loss of 200 kg of waste in waste water and they are currently unutilized (Cabeza et al., 1998). The majority of these solid wastes are generated in pre-tanning operations like pre-fleshing, fleshing, shaving and trimming (Işler et al., 2010). Global production estimate of hides and skins comes around 6.96 million tonnes per annum. It is interesting to note that India processes 700000 tonnes contributing around 70000 tonnes to 100000 tonnes of fleshing waste (Buljan, 1999; FAO, 2016). These waste consist of water (80 %), collagen (8%), salts (8%) and fats (4%) (Nishad Fathima et al., 2014). The current disposal method for fleshing waste is landfilling, which incurs more labor cost and results in severe land pollution.

Components of fleshing waste can be utilized to yield new value-added products for sustainable technologies. Valorization of waste to produce a value-added product will not only reduce the complications of waste management but will also have a positive and significant impact on the economy (Catalina et al., 2012).

There are several reports available in the literature to utilize fleshing waste for the preparation of value-added products. Fleshing waste has been utilized as a potential adsorbent to remove the dyes and chromium (VI) from waste water (Fathima et al., 2011, 2005). The potent usage of fat content from the fleshing waste has resulted in preparation of biodiesel (Alptekin et al., 2012; Özgünay et al., 2007) Yuvaraj et al. prepared activated carbon by the pyrolysis of fleshing waste with the effective employment of activated carbon as an adsorbent for chromium (VI) from waste water (Palani et al., 2017; Yuvaraj et al., 2018). They have also been anaerobically digested for the preparation of biogas (Shanmugam and Horan, 2009). In addition, these fleshing wastes have been vermin composted to the nutrient-enriched product by *Eisenia foetida* (Ravindran et al., 2008).

The commercial feasibility of the above-mentioned product is very low. Therefore, an effective utilization of this solid waste by converting them to value-added materials is the need of the hour. Collagen, a fibrous protein is found to be abundant in fleshing waste. The fibrous nature of collagen can be employed in applications like acoustics, where the fibers enhance the sound absorption. Noise or unwanted sound is said to be a pollutant and an environmental stressor. The obliged noise exposure steers in hearing loss, sleep disturbances resulting in psychological harms (Na et al., 2012; Stansfeld et al., 2000). Sound absorbing materials are effective solutions for this prevalent issue. Sound absorbing materials dissipate more of the incoming sound waves and prevent reflections. Of the different sound absorbing materials, porous materials have a multitude of small openings or pores through which the sound energy is lost by viscous and thermal losses (Bahrambeygi et al., 2013). Nanofibers have gained great attention as absorbing materials because of their porosity and high surface to volume ratio. When the sound wave strikes the surface of the nanofiber membrane, there is a movement in the membrane leading to the conversion of sound energy to kinetic and thermal energy (Mohrova and Kalinova, 2012).

Synthetic sound absorbing materials emits greenhouse gases during the manufacturing process, which led to the use of eco-friendly materials from renewable resources thereby discovering viable alternatives for conventional materials (Arenas and Crocker, 2010). Natural fibers such as cotton, kenaf, coir, hemp, and flax have been used for sound absorption. Use of multiple layered sound absorption materials with these natural fibers can enhance the sound absorption coefficient.

In the present study, extraction of protein hydrolysate from limed fleshing waste and the fabrication of fleshing hydrolysate- PVA nanofibers through co-electrospinning have been attempted. Nanofibers were characterized for their structural, thermal and mechanical properties. The prepared nanofibrous membrane was layered on a coir fiber disc. This bilayer material was characterized for its sound absorption behavior.

2. Experimental

2.1 Materials

Polyvinyl alcohol (MW- 160000 Da) was purchased from Hi-Media. Glacial acetic acid was procured from Merck (98%). Acetone (Commercial grade) was obtained from SRL chemicals. Limed Fleshing waste (Cow, 25 kg) was collected from tannery division of CSIR- CLRI. Coir pith discs were obtained from Manidharma Biotech Pvt Ltd.

2.2 Pre-treatment of fleshing waste

Limed fleshing was washed with water to remove the impurities such as dirt and soluble lime. The fleshings were further delimed with 5% ammonium chloride overnight followed by degreasing with petroleum ether. The fleshings were further dehydrated using increasing concentrations of acetone (10 %, 20 %, 40 %, 80 % and 100 %). Dehydrated samples were vacuum dried at 60°C for 3 hours followed by milling with Wiley mill to prepare fine powder. The prepared fleshing powder was stored for further use.

2.3 Preparation of fleshing hydrolysates

2.5 g of vacuum dried fleshing powder was taken separately in 100 mL of acetic acid in varying molar concentrations (0.5 M, 1 M, 1.5 M, 2 M, and 2.5 M) and stirred at 80ºC for 6 hours. The solutions were centrifuged at 10000 rpm for 30 minutes. The supernatant was collected and the residue was dried at 80 °C to remove the moisture content. The hydrolysate solution was dialyzed extensively against 0.05 M acetic acid for 48 hours to remove the impurities. The solution was further lyophilized to obtain hydrolysate sponges. The experiments were performed in triplicates and the data were expressed as average ± standard deviation.

2.4 Methods

2.4.1 Characterization studies of fleshing hydrolysate

The residual weight after the hydrolysis was estimated and the percentage of hydrolysis was calculated using the following formula.

$$Percentage\ of hydrolysis = \frac{Initial\ weight\ taken\ for\ hydrolysis - Residual\ weight\ after\ hydrolysis}{Initial\ weight\ taken\ for\ hydrolysis} X\ 100$$

Hydroxyproline content in fleshing hydrolysate sponge was estimated by Woessner’s method (Woessner, 1961). 1 mg of fleshing hydrolysate sponge was dissolved in water (1 mg/ 100 µl) followed by complete hydrolysis with an equal volume of 6N HCl at 110 °C for overnight. The samples were dried and made up with known amount of distilled water for performing the assay. Three samples were taken for estimation from each group and the values are expressed as average ± standard deviation. Functional group analysis was carried out using FTIR (Jasco FTIR spectrophotometer) by KBr pellet method and the spectra were recorded between 400- 4000 cm-^{1}.

2.4.2 Electrospinning of PVA- fleshing hydrolysate

Initial optimization for the formation of nanofibers was done by varying the concentrations of PVA and fleshing hydrolysate, applied voltage and tip to collector distance. PVA concentration was varied from 6 %- 8 % whereas voltage was varied from 10- 25 kV and the tip to collector distance varied from 10 cm- 15 cm. It was found that at 6 % and 7 % PVA concentration, beaded nanofibers were produced whereas at 8 % the beadless, smooth and uniform nanofibers were obtained. 8 % PVA and 5 % fleshing hydrolysate was fixed through the above optimization. 200 mg of hydrolysate sponge was dissolved in 4 ml of a binary solvent system consisting of glacial acetic acid-water (1:1) to make 5% solution concentration. To the above solution, PVA was added to make 8 % solution and kept under constant stirring for 90 minutes at 80° C. The solution was electrospun using ESPIN-NANO electrospinning apparatus (India). Briefly, the solution was fed into 2 ml syringe attached with a 24G needle. The flow rate was maintained as 0.5 ml/hr. The distance between the tip of the needle to the collector was maintained as 10 cm. The applied voltage was fixed at 20 kV. These experiments were performed at room temperature.

2.4.3 Characterization studies of nanofibers

Surface morphology of the electrospun nanofibers was characterized using a scanning electron microscope (Hitachi S-3400N, Japan) at an acceleration voltage of 5 kV. Samples were sputter coated with gold before imaging. Average fiber diameter was determined from 100 random measurements per image using ImageJ. ATR-FTIR measurements for the nanofibers were carried out using Jasco ATR-FTIR spectrophotometer in the region of 600-4000 cm^{-1}. All the samples were scanned with the resolution of 4 cm^{-1}. Mechanical properties of the nanofibers were determined using Instron Universal Tensile Tester. Nanofiber mats of dimension, 10 X 50 mm were fixed between two clamps of the instrument for testing and the stroke rate was maintained as 5 mm/min. Triplicates were taken for each sample. Surface area and pore size of the nanofibers was measured by nitrogen adsorption at 77.3 K using surface analyzer (Belsorp-mini II, BEL, Japan). Porosity of the nanofibers was measured using automated humid air porometer (Porous Materials Inc. HCFP-1100-AE). Thickness of the nanofiber membranes was determined using micrometer screw gauge at five different places and the average value was taken. Thermal behavior of the nanofibers was investigated using differential scanning Calorimetry (Netzsch- DSC 204 F1 Phoenix) from temperature 25 °C- 250 °C at the heating rate of 10 °C/min. Thermogravimetric analysis for the nanofibers was performed at a temperature range of 30- 750 °C using Universal V4.4A TA Instruments. The crystallinity of the nanofibers was analyzed using Rigaku Miniflex II desktop X-Ray diffractometer with Cu Kα radiation (λ= 1.540562 Å).

2.4.4 Acoustic absorbance studies

The sound absorption coefficient for the nanofibers was calculated by two microphone impedance tube method (Bruel & Kjaer, Denmark) according to the ISO standard (ISO standard 10534–2, 1998). A large tube (99.5 mm) setup was used to measure the frequency in the range of 100 Hz to 1600 Hz. The nanofibrous mats were prepared with the diameter of 99.5 mm. The mats were placed as a layer on the surface of the coir fiber disc of diameter 99.5 mm (Thickness-15 mm) and the sound absorption was measured. The experiments were performed in triplicates and the results were plotted.

3.0 RESULTS AND DISCUSSIONS

3.1 Percentage of hydrolysis

Hydrolysis percentage was calculated based on the residual weight of the fleshing waste. The process was carried out by maintaining initial weight (2.5 grams), time (6 hrs) and temperature (80°C) as constant with varying concentrations of acetic acid (0.5, 1, 1.5, 2 and 2.5 M). The results are presented in table 1. It was observed that the concentration of acetic acid plays a significant role in the hydrolysis process. Upon increasing the concentration of acetic acid, the percentage of hydrolysis was found to be increasing. The increase in acetic acid concentration attributes to the extensive breakage of amide bonds in fleshings, which leads to the maximum hydrolysis.

Table 1. Percentage of hydrolysis of fleshing waste with different acetic acid concentrations

Concentration of Acetic acid (M)	Percentage of hydrolysis (%)
0.5	48 ± 1.4
1	50.5 ± 13.4
1.5	85.5 ± 3.5
2	87 ± 2.8
2.5	87.5 ± 2.1

3.2 Hydroxyproline Content

Hydroxyproline (HP) is one of the major amino acids present in the collagen protein. Estimation of the hydroxyproline content in the fleshing hydrolysate sponge can elucidate more information about the hydrolyzed protein sample and the estimated HP values are shown in table 2.

The amount of hydroxyproline increases with the increasing concentration of acetic acid for lower concentrations. However, for higher acetic acid concentrations, the amount of hydroxyproline in the sample decreases. At higher concentrations, hydrolysis of the peptide bonds becomes stronger and thus the number of amino acids extracted becomes higher.

However, during the dialysis, there might be a loss of amino acids, which would have contributed to the decrease in the level of HP in hydrolysate (Sompie et al., 2015).

Table 2. Amount of hydroxyproline content in fleshing hydrolysate sponges

Acetic acid concentration (M)	HP Content/ mg of sponge (μg)
0.5	71.98 ± 4.6
1	86.58 ± 3.2
1.5	87.47 ± 3.7
2	77.81 ± 5.1
2.5	66.59 ± 6.4

3.3 Impact of various hydrolysis conditions on the functional groups of hydrolysates

FTIR analysis was performed to identify the impact of hydrolysis on the functional group changes after the hydrolysis process. FTIR spectra of fleshing hydrolysate prepared from the limed fleshings are depicted in figure 1. Fleshing hydrolysates exhibits a less intense peak at amide I around 1611 cm^{-1}, which corresponds to C=O stretching, high intense peak at amide II, which corresponds to out of phase combination of –CN stretching and –NH bending and moderate intense peak at amide III reads for in-phase combination of –CN stretching and –NH bending (Barth, 2007; Kong and Yu, 2007) and the peak positions are presented in table 3.

Amide I peak was found to be around 1608 cm^{-1} and showed a minor variation with different hydrolysis conditions. Since the amide I is more sensitive to the secondary structure of proteins, increasing the acetic acid concentration does not significantly affect the conformation of the polypeptide chains in the protein hydrolysate. Amide II peak was found to be around 1542 cm^{-1} and does not vary notably with different hydrolysis conditions. Amide III peak was found to be increasing towards higher wavelength with the increasing concentration of acetic acid.

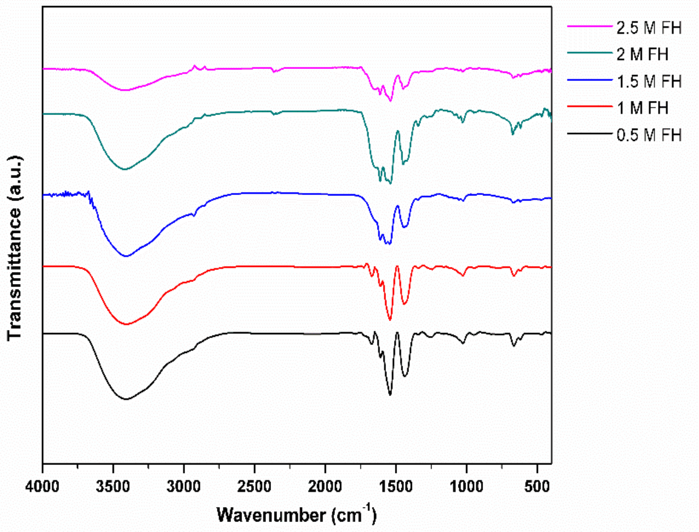

Figure 1. FTIR spectra of fleshing hydrolysate with different hydrolysis conditions

Table 3. Peak positions of fleshing hydrolysate with different hydrolysis conditions

Concentration of acetic acid (M)	Amide I (cm^{-1})	Amide II (cm^{-1})	Amide III (cm^{-1})
0.5	1608	1542	1251
1	1610	1542	1247
1.5	1611	1543	1280
2	1611	1543	1278
2.5	1611	1540	1278

3.4 Characterizations of PVA and PVA- Fleshing hydrolysate nanofibers

3.4.1 Morphological analysis

It is important to prepare highly porous materials for the sound absorption applications, which was obtained through electrospinning. PVA and fleshing hydrolysate were mixed in the ratio of 8:5 to prepare nanofibers. SEM micrographs and the corresponding histograms for the prepared PVA and PVA-fleshing hydrolysate nanofibers are shown in figure 2.

Nanofibers were found to be smooth, beadless, and uniform with highly porous structures. Neat PVA nanofibers showed the fiber diameter around 128 ± 30 nm. The addition of fleshing hydrolysate had increased the diameter of fibers. Upon addition of hydrolysates with varied extraction conditions yielded nanofibers with different diameters. The variation in molecular weight of the hydrolysates due to the different hydrolysis condition plays a role in the fiber diameter variation. The variations in the viscosity and conductivity would have contributed to the change in the diameter of the fiber. Fleshing hydrolysate prepared from higher acetic concentrations forms higher diameter composite nanofibers with PVA (1 M, 1.5 M, 2 M, and 2.5 M) when compared to the neat PVA nanofibers, whereas the hydrolysate prepared from the lower concentration (0.5 M) have decreased the diameter of fibers.

Figure 2. SEM images and the corresponding histograms of nanofibers made of PVA and Fleshing hydrolysate – PVA. (0.5 M Fleshing hydrolysate, 1 M Fleshing hydrolysate, 1.5 M Fleshing hydrolysate, 2 M Fleshing hydrolysate, 2.5 M Fleshing hydrolysate).

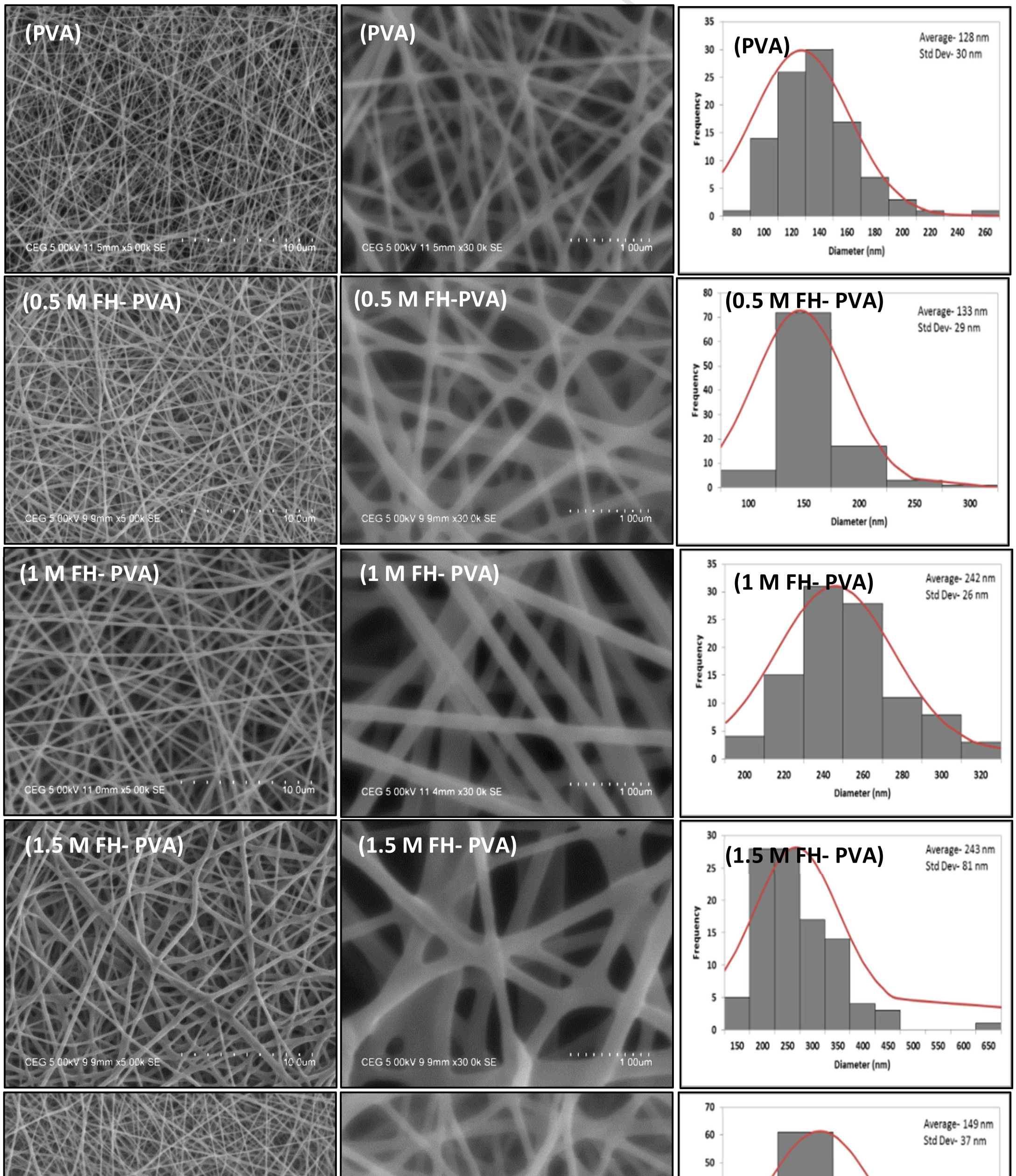
(PVA)
CEG 5.00kV 11.5mm x5.00k SE
10.0um
(PVA)
CEG 5.00kV 11.5mm x30.0k SE
1.00um
(PVA)
Average- 128 nm
Std Dev- 30 nm
Frequency
Diameter (nm)
(0.5 M FH- PVA)
CEG 5.00kV 9.9mm x5.00k SE
10.0um
(0.5 M FH-PVA)
CEG 5.00kV 9.9mm x30.0k SE
1.00um
(0.5 M FH- PVA)
Average- 133 nm
Std Dev- 29 nm
Frequency
Diameter (nm)
(1 M FH- PVA)
CEG 5.00kV 11.0mm x5.00k SE
10.0um
(1 M FH- PVA)
CEG 5.00kV 11.4mm x30.0k SE
1.00um
(1 M FH- PVA)
Average- 242 nm
Std Dev- 26 nm
Frequency
Diameter (nm)
(1.5 M FH- PVA)
CEG 5.00kV 9.9mm x5.00k SE
10.0um
(1.5 M FH- PVA)
CEG 5.00kV 9.9mm x30.0k SE
1.00um
(1.5 M FH- PVA)
Average- 243 nm
Std Dev- 81 nm
Frequency
Diameter (nm)
Average- 149 nm
Std Dev- 37 nm

3.4.2 Functional group analysis

FTIR analysis was performed to find the interaction between PVA and fleshing hydrolysate after electrospinning and the spectra are represented in figure 3. PVA nanofibers exhibited characteristic peaks at 3306 cm^{-1}, which attributes to symmetrical –OH stretching, 2922 cm^{-1} corresponds to –CH$_2$ asymmetric stretching, 1427 cm^{-1} reads for –CH$_2$ bending and 1091 cm^{-1}for C-O-C stretching.

Fleshing hydrolysate- PVA nanofibers showed a minor shift in the –OH stretching peak of PVA and it was found to be around 3318 cm^{-1}. This could be due to the formation of hydrogen bonds between PVA and peptides in the fleshing hydrolysate. The amide I peak for fleshing hydrolysate shows a positive shift in nanofibers around 1646 cm^{-1}, 1649 cm$^{-1,}$ 1644 cm^{-1}, 1649 cm^{-1}and 1649 cm^{-1} for 0.5 M, 1 M, 1.5 M, 2 M and 2.5 M fleshing hydrolysate- PVA nanofibers respectively. This drastic shift in the amide I peak might be owing to the non-covalent interactions between PVA and the peptides in the fleshing hydrolysate. The amide II and amide III peaks showed only a narrow shift in the nanofibers.

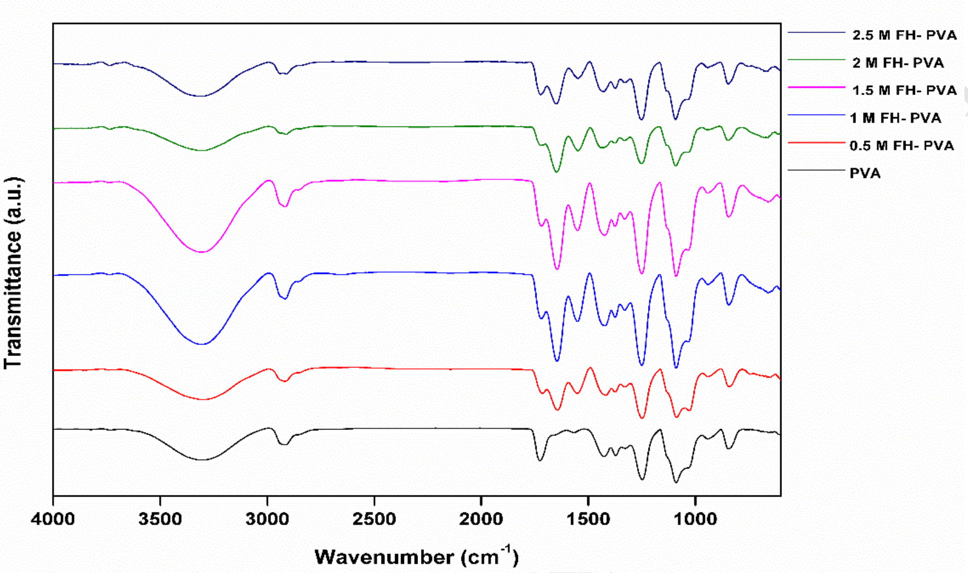

Figure 3. ATR- FTIR spectra of PVA nanofibers and Fleshing hydrolysates- PVA nanofibers (0.5 M Fleshing hydrolysate, 1 M Fleshing hydrolysate, 1.5 M Fleshing hydrolysate, 2 M Fleshing hydrolysate, 2.5 M Fleshing hydrolysate).

3.4.3 Porosity and thickness measurements

Specific surface area of nanofibers by BET analysis is shown in table 4. It was found that the specific surface of area of PVA nanofibers is 4.19 m^2/g. However, the specific surface area of nanofibers decreases to 2.97 m^2/g after the incorporation of fleshing hydrolysate. The surface area is decreased because of the higher fiber diameter of fleshing hydrolysate incorporated nanofibers when compared to the pure PVA nanofibers. Thickness of the PVA nanofibers was found to be 153 ± 31 µm whereas thickness of the 2.5 M fleshing hydrolysate incorporated PVA nanofibers was found to be 261 ± 38 µm. These nanofiber layers were placed on the surface of coir disc of thickness 15 mm. Pore size distribution of the PVA nanofibers and fleshing hydrolysate- PVA nanofibers is shown in figure 4 and 5. It was found that the PVA nanofibers showed the pore size diameter between 0.1 to 0.47 µm. However, the pore size distribution reduced between 0.12 to 0.23 µm for fleshing hydrolysate- PVA nanofibers.

Table 4. Specific surface area of PVA nanofibers and 2.5 M fleshing hydrolysate- PVA nanofibers

Material	**Specific surface area (m^2/g)**	**Mean pore diameter (nm)**	**Total pore volume (cm^3/g)**
PVA nanofibers	4.19	6.26	6.56
2.5 M fleshing hydrolysate- PVA nanofibers	2.97	5.9	4.36

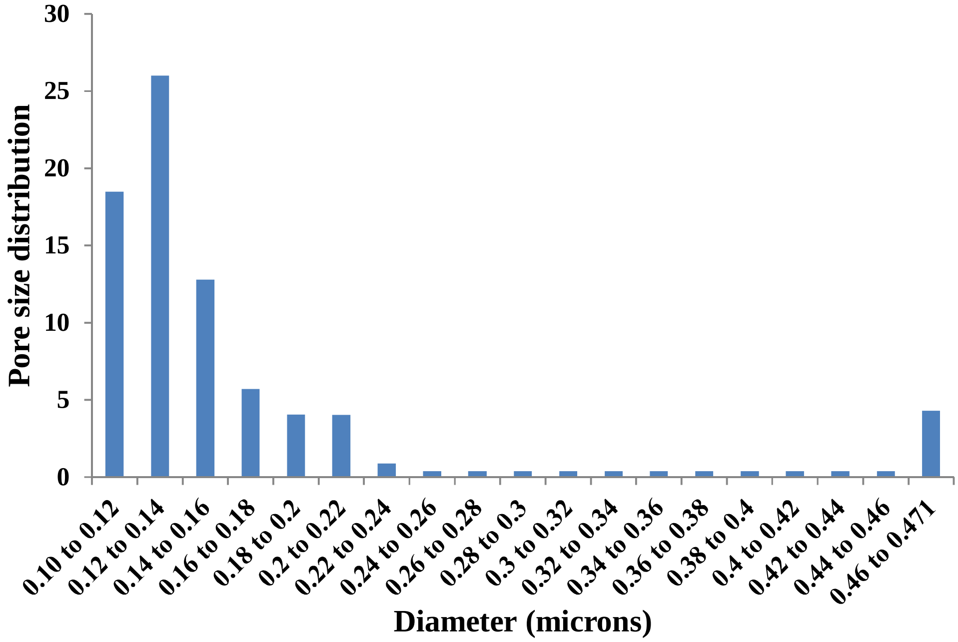

Figure 4. Pore size distribution of PVA nanofibers

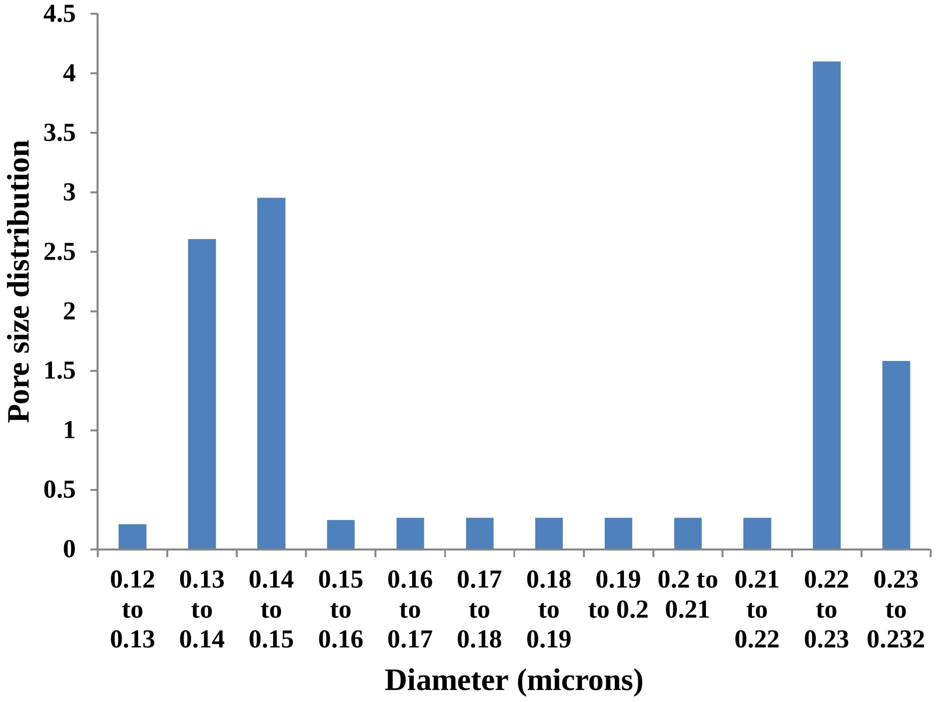

Figure 5. Pore size distribution of 2.5 M fleshing hydrolysate- PVA nanofibers

3.4.4 XRD analysis

XRD analysis was performed to examine the influence of fleshing hydrolysate on the crystal structure of PVA and XRD spectra of nanofibers are shown in figure 6. PVA nanofibers exhibited a single peak around 20° C, which corresponds to (101) semi-crystalline peak of PVA. However, the peak has broadened and it has shown lesser intensity in fleshing hydrolysate- PVA nanofibers. The hydroxyl group in PVA side chain is held responsible for its crystallinity (Shao et al., 2003). In Fleshing hydrolysate- PVA nanofibers, the OH groups might have involved in the hydrogen bonding with the peptides of the hydrolysate, which have reduced the crystallinity of the PVA contributing to the peak broadening.

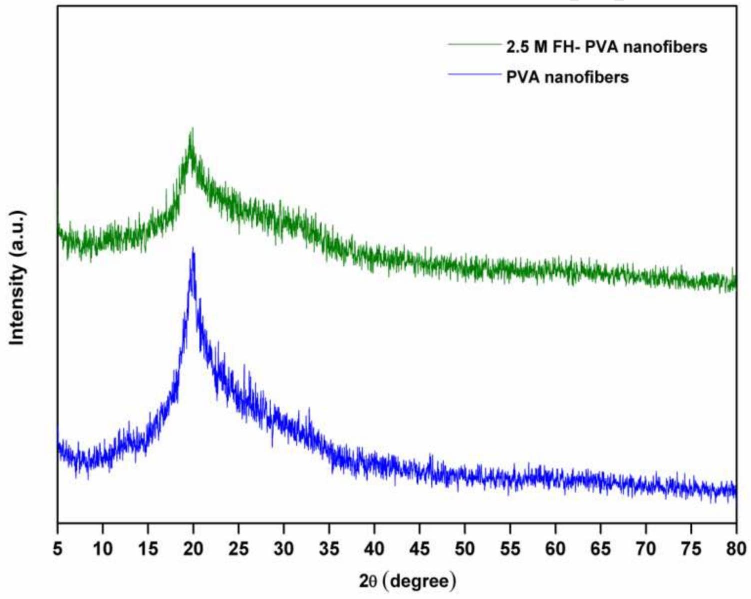

Figure 6. XRD spectra of PVA nanofibers and 2.5 M Fleshing hydrolysate- PVA nanofibers

3.4.5 Thermal stability analysis

TGA and DSC analysis for nanofibers were performed to investigate the thermal properties and the results are shown in figure 7 and 8.

TGA curves for both PVA and fleshing hydrolysate- PVA nanofibers are shown in figure 7 and the corresponding DTG curves are shown in figure 8. PVA nanofibers decompose in a three-step process, whereas for fleshing hydrolysate- PVA nanofibers the degradation takes place in two steps. PVA nanofibers showed initial weight loss till 80 °C, which could be due to the glass transition and evaporation of moisture from the sample. The major decomposition occurred during the second degradation step starts around 260 °C and the nanofibers showed nearly 78% mass loss at 334 °C, which is mainly due to the degradation of the side chains of PVA. The third degradation took place around 480 °C, which attributes to the degradation of the main chains of PVA (Santos et al., 2014).

Fleshing hydrolysate- PVA nanofibers showed initial weight loss till 80°C due to the moisture loss. For 0.5 M, 1 M, 1.5 M, 2 M, 2.5 M FH- PVA nanofibers, the major degradation starts at 258 °C, 274 °C, 274.5 °C, 267 °C and 260 °C respectively. The maximum degradation of PVA occurs at 304 °C, whereas the value increased upto 315 °C for fleshing hydrolysate- PVA nanofibers. The hydrogen bonding interactions between – OH groups of PVA and peptides of fleshing hydrolysate could be possible reason for the increase in degradation temperature, thereby it enhancing the thermal stability of the nanofiber mats.

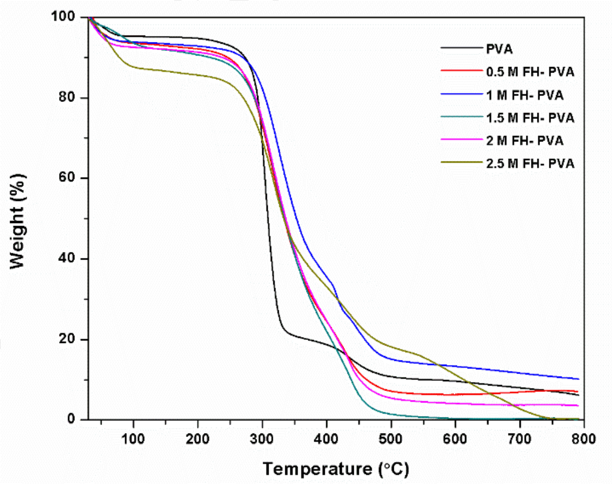

Figure 7. TGA thermograms of electrospun PVA nanofibers and Fleshing Hydrolysate- PVA nanofibers. (0.5 M Fleshing hydrolysate, 1 M Fleshing hydrolysate, 1.5 M Fleshing hydrolysate, 2 M Fleshing hydrolysate, 2.5 M Fleshing hydrolysate)

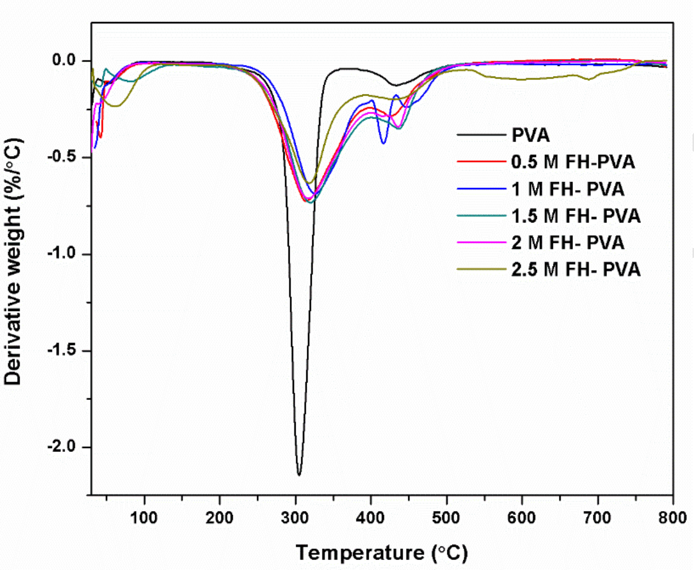

Figure 8. DTG thermograms of electrospun PVA nanofibers and Fleshing Hydrolysate- PVA nanofibers. (0.5 M Fleshing hydrolysate, 1 M Fleshing hydrolysate, 1.5 M Fleshing hydrolysate, 2 M Fleshing hydrolysate, 2.5 M Fleshing hydrolysate)

DSC curves of PVA and Fleshing hydrolysate- PVA nanofibers are shown in figure 9. PVA nanofibers showed moisture loss along with glass transition temperature around 40 to 110°C (Santos et al., 2014) . In PVA- Fleshing hydrolysate composite nanofibers, the addition of fleshing hydrolysate have increased the glass transition temperature of PVA from 54 to 66°C varying for various hydrolysates. Pure PVA nanofibers showed melting point at 192°C. However, the addition of fleshing hydrolysate lowers the melting point of PVA from 182 to 190°C. PVA is said to be semi-crystalline polymer with highly ordered structure. The presence of hydrolysate peptides might have decreased the ordered association of PVA molecules, which inturn reduces the melting temperature of the fleshing hydrolysate- PVA nanofibers.

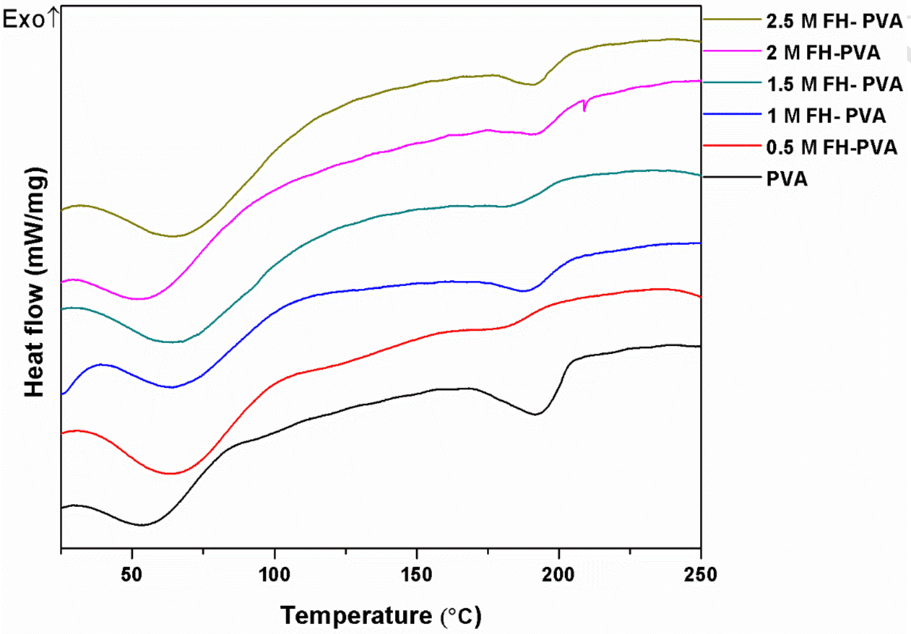

Figure 9. DSC thermograms of electrospun PVA nanofibers and Fleshing Hydrolysate- PVA nanofibers (0.5 M Fleshing hydrolysate, 1 M Fleshing hydrolysate, 1.5 M Fleshing hydrolysate, 2 M Fleshing hydrolysate, 2.5 M Fleshing hydrolysate).

3.4.6 Mechanical strength analysis

The effect of fleshing hydrolysate on the tensile strength of PVA nanofibers was studied and the results are shown in figure 10. PVA nanofibers showed the tensile strength around 0.6 MPa. Fleshing hydrolysate- PVA nanofibers exhibited significantly higher tensile strength than PVA nanofibers, which could be due to the formation of hydrogen bonding between the hydroxyl groups of PVA and amino groups of fleshing hydrolysate. Among the fleshing hydrolysate – PVA nanofibers, 0.5 M nanofibers showed better tensile strength. At 0.5 M acetic acid concentration the extent of hydrolysis is less hence could result in higher molecular weight peptides, which might have contributed for the increase in tensile strength. However, when the acid concentration gets increased, hydrolysis increases leading to smaller peptide fragments, which should result in lower tensile strength. But an increase in tensile strength is observed which could be due to the orientation of the peptides along the axis of nanofibers during the electrospinning process and this might have contributed for the slight enhancement in tensile strength.

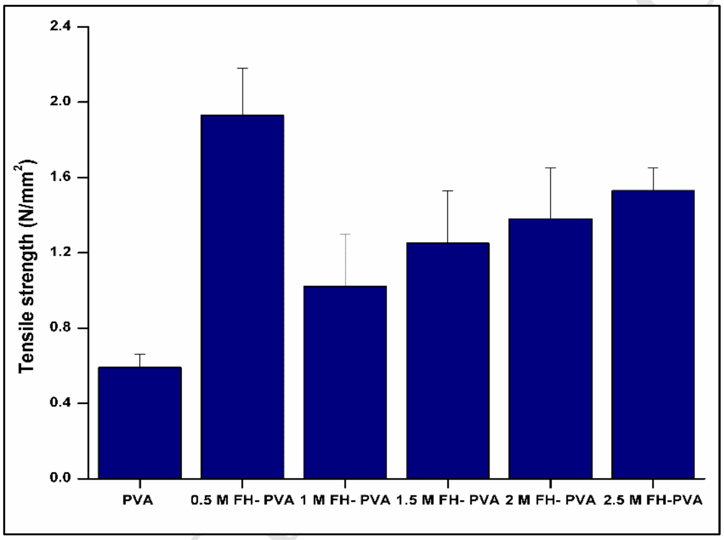

Figure 10. Tensile strength of the electrospun PVA nanofibers and fleshing hydrolysate- PVA nanofibers (0.5 M Fleshing hydrolysate, 1 M Fleshing hydrolysate, 1.5 M Fleshing hydrolysate, 2 M Fleshing hydrolysate, 2.5 M Fleshing hydrolysate)

3.5 Sound absorption coefficient of the nanofibrous mats layered on coir disc

The sound absorption coefficient of the coir disc and the bilayered material consisting of coir disc and nanofibers were measured using impedance tube method and the results are shown in figure 11. Coir showed better sound absorption peak around 1000- 1600 Hz. However, upon the application of nanofibers, the sound absorption peak decreased towards the lower frequency viz. 1000- 1600 Hz. Whereas, the fleshing hydrolysate- PVA nanofibers with coir showed maximum sound absorption peak in the frequency range of 200- 1000 Hz than the pure coir and PVA nanofiber-coir materials. Thickness, surface area and porosity are the various factors which affects the sound absorption efficiency (Seddeq, 2009). Thickness of the sound absorbing material affects the sound absorption co-efficient in the lower frequencies. Since the thickness of the FH- PVA nanofiber mats is higher than the PVA nanofibers, the layering of FH incorporated nanofibers on the surface of nanofibers might have increased the sound absorption co-efficient. The nanofibers provided higher surface area for the sound waves to interact with the nanofibers resulting in the vibration of nanofibers leading to the energy dissipation. Nanofibers have shown greater porosity for the sound waves to pass through and also they can move easily during the interaction with the sound waves than the fibers with higher diameter leading to more energy loss. For higher frequencies, the nanofibers become reflective to the sound waves, thereby movement of sound waves interaction becomes less thereby leading to the lesser energy loss leading to minimum sound absorption (Seddeq, 2009; Wu and Chou, 2016). So, the reflective nature of nanofibers might have decreased the sound absorption of nanofibers layered coir materials in the frequency range 1000 Hz- 1600 Hz. The sound absorption behavior of our bilayer material is higher when compared with non-oven with polyacrylonitrile nanofibers and non-oven with polyurethane nanofibers over the frequency range 100 Hz- 1000 Hz reported in the literature (Rabbi et al., 2014). Thus, the fleshing hydrolysate- PVA nanofibers layered on the coir disc is the favorable material for lower frequency noise reduction.

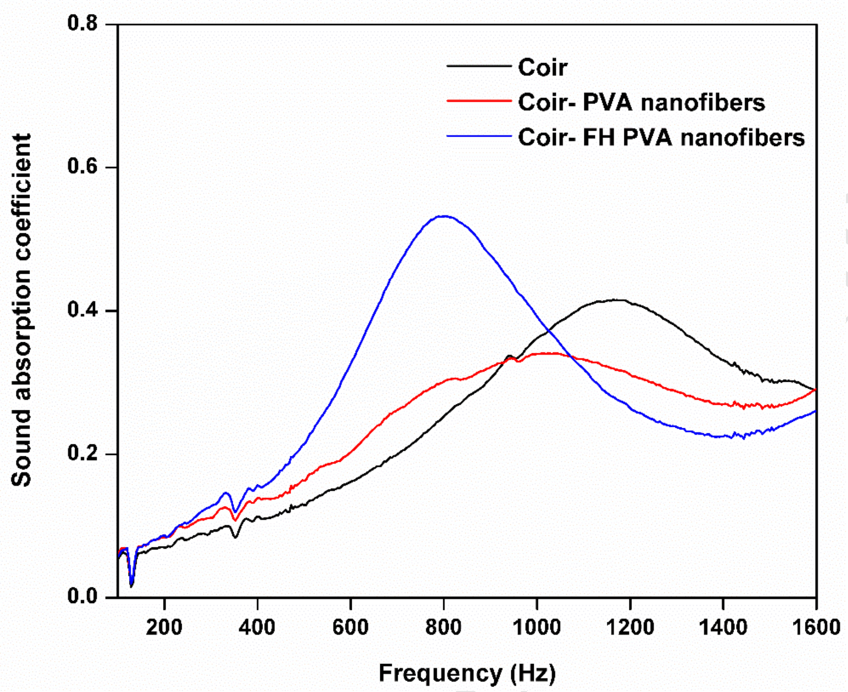

Figure 11. Sound absorption efficiency of Coir, PVA Nanofiber - Coir and Fleshing hydrolysate-PVA nanofibers – Coir materials

CONCLUSION

In the current study, fleshing hydrolysate was prepared from limed fleshing waste and fleshing hydrolysate- PVA nanofibers were successfully prepared by electrospinning technique. Hydrolysis yield was found to be increasing with the increase in concentration of acetic acid. FTIR and TGA studies revealed that there were strong molecular interactions between fleshing hydrolysates and PVA. Fleshing hydrolysate enhances thermal stability of the PVA nanofibers by increasing its decomposition temperature. The bilayer composed of fleshing hydrolysate-PVA nanofibers and coir disc showed better sound absorption at lower frequencies when compared to pure coir materials. Thus, this novel sustainable technology might produce an excellent sound absorbing material and it will replace the existing solid waste management technologies in leather industry.

Funding Sources

This work was financially supported by Department of Biotechnology, Government of India. (Grant Number- BT/PR4406/NNT/28/574/2011).

REFERENCES

Alptekin, E., Canakci, M., Sanli, H., 2012. Evaluation of leather industry wastes as a feedstock for biodiesel production. Fuel 95, 214–220. https://doi.org/10.1016/j.fuel.2011.08.055

Arenas, J.P., Crocker, M.J., 2010. Recent Trends in Porous Sound-Absorbing Materials. Sound Vib. 12–17.

Bahrambeygi, H., Sabetzadeh, N., Rabbi, A., Nasouri, K., Shoushtari, A.M., Babaei, M.R., 2013. Nanofibers (PU and PAN) and nanoparticles (Nanoclay and MWNTs) simultaneous effects on polyurethane foam sound absorption. J. Polym. Res. 20. https://doi.org/10.1007/s10965-012-0072-6

Barth, A., 2007. Infrared spectroscopy of proteins. Biochim. Biophys. Acta - Bioenerg. 1767 (9), 1073-1101. https://doi.org/10.1016/j.bbabio.2007.06.004

Buljan, J., 1999. Application of fleshing to upflow anaerobic sludge blanket reactor for biogas generation at CLRI, Chennai, INDIA.

Cabeza, L.F., Taylor, M.M., Dimaio, G.L., Brown, E.M., Marmer, W.N., Carrió, R., Celma, P.J., Cot, J., 1998. Processing of leather waste: Pilot scale studies on chrome shavings. Isolation of potentially valuable protein products and chromium. Waste Manag. 18, 211–218. https://doi.org/10.1016/S0956-053X(98)00032-4

Catalina, M., Cot, J., Balu, A.M., Serrano-Ruiz, J.C., Luque, R., 2012. Tailor-made biopolymers from leather waste valorisation. Green Chem. 14, 308-312. https://doi.org/10.1039/c2gc16330f

FAO, 2016. World Statistical Compendium for raw hides and skins, leather and leather footwear

1999-2015, Trade and Markets Division.

Fathima, N.N., Aravindhan, R., Rao, J.R., Nair, B.U., 2011. Stabilized protein waste as a source for removal of color from wastewaters. J. Appl. Polym. Sci. 120, 1397–1402. https://doi.org/10.1002/app.32884

Fathima, N.N., Aravindhan, R., Rao, J.R., Nair, B.U., 2005. Solid waste removes toxic liquid waste: Adsorption of chromium(VI) by iron complexed protein waste. Environ. Sci. Technol. 39, 2804–2810. https://doi.org/10.1021/es0499389

Işler, A., Sundu, S., Tüter, M., Karaosmanoĝlu, F., 2010. Transesterification reaction of the fat originated from solid waste of the leather industry. Waste Manag. 30, 2631–2635. https://doi.org/10.1016/j.wasman.2010.06.005

ISO standard 10534–2, 1998. Acoustics determination of sound absorption coefficient and impedance in impedance tube Part 2: Transfer function method.

Kong, J., Yu, S., 2007. Fourier transform infrared spectroscopic analysis of protein secondary structures. Acta Biochim. Biophys. Sin. (Shanghai). 39, 549–559. https://doi.org/10.1111/j.1745-7270.2007.00320.x

Mohrova, J., Kalinova, K., 2012. Different structures of PVA nanofibrous membrane for sound absorption application. J. Nanomater. 2012 (11). https://doi.org/10.1155/2012/643043

Na, Y., Agnhage, T., Cho, G., 2012. Sound absorption of multiple layers of nanofiber webs and the comparison of measuring methods for sound absorption coefficients. Fibers Polym. 13, 1348–1352. https://doi.org/10.1007/s12221-012-1348-5

Nishad Fathima, N., Raghava Rao, J., Unni Nair, B., 2014. Chapter 23 – Effective Utilization of

Solid Waste from Leather Industry, in: The Role of Colloidal Systems in Environmental Protection. 593–613. https://doi.org/10.1016/B978-0-444-63283-8.00023-5

Özgünay, H., Çolak, S., Zengin, G., Sari, Ö., Sarikahya, H., Yüceer, L., 2007. Performance and emission study of biodiesel from leather industry pre-fleshings. Waste Manag. 27, 1897–1901. https://doi.org/10.1016/j.wasman.2006.08.014

Palani, Y., Rao Jonnalagadda, R., Fathima Nishter, N., 2017. Adsorption on activated carbon derived from tannery fleshing waste: Adsorption isotherms, thermodynamics, and kinetics. Environ. Prog. Sustain. Energy 36, 1725–1733. https://doi.org/10.1002/ep.12637

Ravindran, B., Dinesh, S.L., Kennedy, L.J., Sekaran, G., 2008. vermicomposting of solid waste generated from leather industries using epigeic earthworm eisenia foetida. Appl. Biochem. Biotechnol. 151, 480–488. https://doi.org/10.1007/s12010-008-8222-3

Rabbi, A., Bahrambeygi, H., Nasouri, K., Shoushtari, A. M., Babaei, M. R. 2014. Manufacturing of PAN or PU Nanofiber Layers/PET Nonwoven Composite as Highly Effective Sound Absorbers. Adv. Polym. Technol., 33, 21425. https://doi.org/10.1002/adv.21425

Santos, C., Silva, C.J., Büttel, Z., Guimarães, R., Pereira, S.B., Tamagnini, P., Zille, A., 2014. Preparation and characterization of polysaccharides/PVA blend nanofibrous membranes by electrospinning method. Carbohydr. Polym. 99, 584–592. https://doi.org/10.1016/j.carbpol.2013.09.008

Seddeq, H.S., 2009. Factors Influencing Acoustic Performance of Sound Absorptive Materials. Aust. J. Basic Appl. Sci. 3, 4610–4617.

Shanmugam, P., Horan, N.J., 2009. Optimising the biogas production from leather fleshing waste by co-digestion with MSW. Bioresour. Technol. 100, 4117–4120. https://doi.org/10.1016/j.biortech.2009.03.052

Shao, C., Kim, H.Y., Gong, J., Ding, B., Lee, D.R., Park, S.J., 2003. Fiber mats of poly(vinyl alcohol)/silica composite via electrospinning. Mater. Lett. 57, 1579–1584. https://doi.org/10.1016/S0167-577X(02)01036-4

Sompie, M., Surtijono, S.E., Pontoh, J.H.W., Lontaan, N.N., 2015. The Effects of Acetic Acid Concentration and Extraction Temperature on Physical and Chemical Properties of Pigskin Gelatin. Procedia Food Sci. 3, 383–388. https://doi.org/10.1016/j.profoo.2015.01.042

Stansfeld, S., Haines, M., Brown, B., 2000. Noise and health in the urban environment. Rev. Environ. Health 15, 43–82. https://doi.org/10.1515/REVEH.2000.15.1-2.43

Woessner, J.F., 1961. The determination of hydroxyproline in tissue and protein samples containing small proportions of this imino acid. Arch. Biochem. Biophys. 93, 440–447. https://doi.org/10.1016/0003-9861(61)90291-0

Wu, C.M., Chou, M.H., 2016. Polymorphism, piezoelectricity and sound absorption of electrospun PVDF membranes with and without carbon nanotubes. Compos. Sci. Technol. 127, 127–133. https://doi.org/10.1016/j.compscitech.2016.03.001

Yuvaraj, P., Rao, J.R., Fathima, N.N., Natchimuthu, N., Mohan, R., 2018. Complete replacement of carbon black filler in rubber sole with CaO embedded activated carbon derived from tannery solid waste. J. Clean. Prod. 170, 446–450. https://doi.org/10.1016/j.jclepro.2017.09.188

Highlights

- An environmental friendly and value added tannery solid waste management approach was developed.
- Protein hydrolysate was prepared from tannery fleshing waste and blended with poly vinyl alcohol to form nanofibers.
- The nanofibrous mat was placed as a layer on the coir fiber disc and the bilayer material showed enhanced sound absorption in the lower frequencies (100- 1000 Hz) when compared to coir.
- This bilayer material can be an effective alternative for synthetic sound absorbing materials.